

Contents lists available at [ScienceDirect](http://www.sciencedirect.com)

Chemical Engineering Research and Design

|ChemE

journal homepage: www.elsevier.com/locate/cherd

A model-based control framework for industrial batch crystallization processes

A. Mesbah^{a,b,*}, J. Landlust^c, A.E.M. Huesman^a, H.J.M. Kramer^b,
P.J. Jansens^b, P.M.J. Van den Hof^a

^a Delft Center for Systems and Control, Delft University of Technology, Mekelweg 2, 2628 CD Delft, The Netherlands

^b Process and Energy Laboratory, Delft University of Technology, Leeghwaterstraat 44, 2628 CA Delft, The Netherlands

^c IPCOS BV, Bosscheweg 135b, 5282 WV Boxtel, The Netherlands

ABSTRACT

Dynamic optimization is applied for throughput maximization of a semi-industrial batch crystallization process. The control strategy is based on a non-linear moment model. The dynamic model, consisting of a set of differential and algebraic equations, is optimized using the simultaneous optimization approach in which all the state and input trajectories are parameterized. The resulting problem is subsequently solved by a non-linear programming algorithm.

The optimal operation is realized by manipulation of the heat input to the crystallizer such that a maximal allowable crystal growth rate is maintained in the course of the process. Effective control of the crystal growth rate in batch crystallization processes is often crucial to avoid product quality degradation. To be able to effectively track the maximum crystal growth rate, the optimal heat input profile is computed on-line using the current system states that are estimated by an extended Luenberger-type observer based on CSD measurements. The feedback structure of the control framework enables the optimizer to reject process uncertainties and account for plant-model mismatch. It is demonstrated that the application of the proposed on-line optimization strategy leads to a substantial increase, i.e. 30%, in the amount of crystals produced at the batch end, while the product quality requirements are fulfilled.

© 2009 The Institution of Chemical Engineers. Published by Elsevier B.V. All rights reserved.

Keywords: Batch process; Crystallization; Seeding; Dynamic optimization; Real-time control; Observer

1. Introduction

Batch crystallization processes are of paramount importance in the production of pharmaceuticals, food and specialty chemicals in the highly competitive chemical industry. Due to low-volume and high-value of such chemicals, interest in the optimal operation of batch crystallization processes has substantially grown in recent years. The main operational challenge in these processes is to increase the productivity while satisfying the product quality and batch reproducibility requirements.

The control of batch crystallization processes is conventionally performed by manipulating the supersaturation trajectory due to its relationship with the fundamental crys-

tallization phenomena, e.g. nucleation, growth, etc. The supersaturation level is normally kept low, well within the metastable region to be able to better fulfill the product quality specifications, namely the purity of crystals, crystal habit and crystal size distribution (CSD). There is a wealth of literature on the improved operation of cooling batch crystallization that mainly concerns the implementation of programmed cooling profiles (Mullin and Nyvlt, 1971; Mayrhofer and Nyvlt, 1988). This is however inadequate if the process productivity is to be increased since low levels of supersaturation hinder the throughput maximization due to minimal crystal growth rates.

In order to alleviate the foregoing deficiency of conventional control policies, a trade-off between the maximization

* Corresponding author at: Delft Center for Systems and Control, Delft University of Technology, Mekelweg 2, 2628 CD Delft, The Netherlands.

E-mail address: ali.mesbah@tudelft.nl (A. Mesbah).

Received 12 December 2008; Received in revised form 3 September 2009; Accepted 24 September 2009

0263-8762/\$ – see front matter © 2009 The Institution of Chemical Engineers. Published by Elsevier B.V. All rights reserved.
doi:10.1016/j.cherd.2009.09.010

Nomenclature

B_0	total rate of nucleation ($\# \text{m}^{-3} \text{s}^{-1}$)
C	solute concentration ($\text{kg}_{\text{solute}} \text{kg}_{\text{solution}}^{-1}$)
C^*	saturation concentration ($\text{kg}_{\text{solute}} \text{kg}_{\text{solution}}^{-1}$)
F_p	product flow rate ($\text{m}^3 \text{s}^{-1}$)
G	crystal growth rate (m s^{-1})
G_{max}	maximum crystal growth rate (m s^{-1})
g	growth rate exponent
H	specific enthalpy (kJ kg^{-1})
K_V	volumetric shape factor
k_b	nucleation rate constant ($\# \text{m}^{-4}$)
k_g	growth rate constant (m s^{-1})
k_1	constant coefficient
k_2	constant coefficient
L	crystal size (m)
m_i	i th moment of the crystal size distribution ($\# \text{m}^i \text{m}^{-3}$)
n	number density ($\# \text{m}^{-3} \text{m}^{-1}$)
Q	heat input (kW)
t	time (s)
t_f	final batch time (s)
V	crystallizer volume (m^3)
x_{est}	estimated system states
y_{meas}	measured process outputs
<i>Greek letter</i>	
ρ	density (kg m^{-3})
<i>Subscripts</i>	
c	crystal
L	liquid
pv	process value
sp	set-point
v	vapor

of batch throughput and the achievement of sufficient product quality has to be sought by satisfying various constraints defined on the supersaturation level and most likely other process inputs and outputs. The control problem of a batch crystallizer is therefore well suited for a model-based control approach by means of dynamic optimization.

In the past decade, the use of dynamic optimization for model-based control applications has received considerable attention in the light of the emergence of computationally powerful modelling and optimization tools, as well as more efficient dynamic optimization approaches. The current practice however favors the open-loop implementation of off-line optimized profiles (Miller and Rawlings, 1994; Lang et al., 1999; Hu et al., 2005; Nowee et al., 2007). This is not an effective optimal control strategy as the performance of the off-line optimized profiles is often deteriorated due to plant-model mismatch, unmeasured process disturbances and irreproducible start-ups, i.e. unknown initial conditions.

To be able to effectively cope with the inherent shortcomings of the open-loop control strategy, the optimal operating policies can be computed in an on-line mode, the so-called closed-loop control strategy. Contrary to the open-loop optimal control, there are only few studies on the latter control strategy reported in the literature (Xie et al., 2001; Zhang and Rohani, 2003; Shi et al., 2006). In these studies, an optimization-based strategy in conjunction with a state esti-

mator is utilized to compute the optimal operating policy in a feedback control framework where the effects of the plant-model mismatch and process uncertainties are accounted for by continuous state adaptation. However, neither of the abovementioned studies experimentally verifies the viability of real-time dynamic optimization of the batch crystallization process under investigation.

Recently, Mesbah et al. (2008) and Landlust et al. (2008) devised model-based feedback control systems on the basis of a sequential dynamic optimizer and a non-linear model predictive controller, respectively, and demonstrated their feasibility for real-time applications. Sequel to our preceding work, this study concerns the development of a simultaneous dynamic optimizer which is embedded in a similar model-based feedback control system. The performance of the control strategy is examined by several open-loop and closed-loop implementations on a semi-industrial fed-batch evaporative crystallizer. It is worth noting that the major advantage of the simultaneous optimization approach over the sequential optimization approach is its superior computational efficiency.

In what follows, Section 2 describes the seeded fed-batch evaporative crystallization process at hand, followed by Section 3 in which the process model for an ammonium sulphate–water system is discussed. In Section 4, the description of the feedback control structure, as well as the formulation of the dynamic optimization problem is given. Section 5 discusses the model validation and the experimental implementation of the proposed control strategy, followed by the concluding remarks outlined in Section 6.

2. Process description

The fed-batch evaporative crystallization of an ammonium sulphate–water system is performed in a 75-l draft tube crystallizer. The crystallizer can be considered as a single perfectly mixed compartment with one inlet and two outlet streams. The fed-batch operation is exercised to compensate for losses in the crystallizer volume due to the evaporation of solvent, i.e. water, and the slurry sampling. The crystallizer is therefore continuously fed throughout the batch experiment with a crystal-free feed stream containing saturated ammonium sulphate solution at 50 °C since the crystallization is carried out isothermally at this temperature. The outlet flows from the crystallizer on the other hand include the unclassified product removal stream, as well as the vapor stream that is free from crystal and solute. The small product flow is withdrawn from the crystallizer at regular time intervals and diluted with the saturated feed solution to facilitate on-line measurement of the CSD with a laser diffraction instrument (HELOS-Vario, Sympatec, Germany).

In order to ensure the reproducibility of batches and achievement of the desired product specifications, seeded batch experiments are carried out. Ground seeds are prepared by milling and sieving of the commercial product crystals of ammonium sulphate (DSM, The Netherlands) to collect 0.6 kg of the 90–125 μm sieve fraction. The seed crystals are aged for 1 h in a saturated solution of ammonium sulphate in a seeding vessel at 50 °C prior to insertion into the crystallizer (Kalbasenka et al., 2007). An in-line concentration measuring probe (LiquiSonic[®], SensoTech, Germany) is utilized to detect the predetermined supersaturation level at which the ground seeds are introduced to the vessel.

3. Crystallization model

The cornerstone of a model-based control strategy is its dynamic process model, describing the dynamic relation between the relevant inputs and outputs of the system to be controlled. Such control strategies utilize the model to continuously explore the degrees of freedom of the process in order to achieve the maximum performance in accordance with an optimization criterion.

The dynamic behavior of a crystallization process can be rigorously captured by a population balance equation, along with conservation equations and kinetic relations. Under the assumptions of perfectly mixed suspension, constant crystallizer volume, nucleation of crystals of infinitesimal size, negligible breakage and agglomeration and size-independent growth of crystals, the population balance equation for a fed-batch process is expressed as

$$\frac{\partial n(t, L)}{\partial t} = -G \frac{\partial n(t, L)}{\partial L} - \frac{F_p}{V} n(t, L) \quad (1)$$

with the following initial and boundary conditions

$$n(0, L) = n_0(L) \quad (2)$$

$$n(t, 0) = \frac{B_0}{G} \quad (3)$$

In Eq. (1) n represents the number density ($\# \text{ m}^{-3} \text{ m}^{-1}$), G is the crystal growth rate (m s^{-1}), B_0 is the total rate of nucleation ($\# \text{ m}^{-3} \text{ s}^{-1}$), L is the characteristic length of crystals (m), V is the crystallizer volume (m^3) and F_p is the unclassified product removal flow rate ($\text{m}^3 \text{ s}^{-1}$).

As is evident from Eq. (1), the population balance equation is a hyperbolic partial differential equation whose accurate numerical solution is often computationally too involved. Moreover, the population balance modelling approach typically leads to a highly complex model describing the evolution of the CSD in a great detail that is not necessarily needed for control applications. The method of moments (Randolph and Larson, 1971) is therefore applied to Eq. (1) in order to recast the population balance equation into a set of computationally affordable reduced-order ordinary differential equations. Upon multiplying both sides of Eq. (1) by $L^i dL$ and integrating over the entire crystal size domain, the following set of differential equations that describes the evolution of moments of the CSD in time is obtained

$$\frac{dm_i}{dt} = 0^i \cdot B_0 + i \cdot G m_{i-1} - \frac{m_i F_p}{V} \quad i = 0, \dots, 4 \quad m_i(0) = m_{i,0} \quad (4)$$

Eq. (4), which that is known as the moment model, provides an exact solution to the population balance equation given in Eq. (1). It however reduces the level of detail of the population balance modelling approach since only certain properties of the crystal population are described, rather than the entire crystal size distribution.

Due to the dependence of the crystallization phenomena on the evolution of supersaturation in the course of the batch process, Eq. (4) has to be coupled with conservation laws. Owing to the isothermal operation of the crystallizer, the mass and energy balance equations simplify to a single expression for the solute concentration

$$\frac{dC}{dt} = \frac{F_p(C^* - C)/V + 3K_V G m_2(k_1 + C)}{1 - K_V m_3} + \frac{k_2 Q}{1 - K_V m_3} \quad C(0) = C_0 \quad (5)$$

where Q is the heat input to the crystallizer (kW), K_V is the crystal volumetric shape factor, C^* is the saturation concentration ($\text{kg}_{\text{solute}} \text{ kg}_{\text{solution}}^{-1}$) and the constant coefficients k_1 and k_2 are given by

$$k_1 = \frac{H_V C^*}{H_V - H_L} \left(\frac{\rho_c}{\rho_L} - 1 + \frac{\rho_L H_L - \rho_c H_c}{\rho_L H_V} \right) - \frac{\rho_c}{\rho_L} \quad \text{and} \quad (6)$$

$$k_2 = \frac{C^*}{V \rho_L (H_V - H_L)}$$

In addition to the first five leading moments of the CSD and the solute concentration balance, kinetic relations should be used to express the crystallization phenomena. Due to the lack of detailed knowledge about the crystallization phenomena taking place in such processes and for the sake of simplicity often required for control applications, the total nucleation rate B_0 and the size-independent crystal growth rate G are modelled by means of empirical power law expressions

$$B_0 = k_b m_3 G \quad (7)$$

$$G = k_g (C - C^*)^g \quad (8)$$

The parameters of the empirical equations are estimated using a set of experimental data of normal batch operation. The physical properties of the ammonium sulphate–water crystallizing system, as well as the nucleation and growth rate kinetic parameters are listed in Table 1.

Table 1 – Model parameters.

Symbol	Parameter	Value	Unit
C^*	Saturation concentration	0.46	$\text{kg}_{\text{solute}} \text{ kg}_{\text{solution}}^{-1}$
g	Growth rate exponent	1	–
H_c	Specific enthalpy of crystals	60.75	kJ kg^{-1}
H_L	Specific enthalpy of liquid	69.86	kJ kg^{-1}
H_V	Specific enthalpy of vapor	2.59×10^3	kJ kg^{-1}
K_V	Volumetric shape factor	0.43	–
k_b	Nucleation rate constant	1.02×10^{14}	$\# \text{ m}^{-4}$
k_g	Growth rate constant	7.50×10^{-5}	m s^{-1}
F_p	Product flow rate	1.73×10^{-6}	$\text{m}^3 \text{ s}^{-1}$
V	Crystallizer volume	7.50×10^{-2}	m^3
ρ_c	Crystal density	1767.35	kg m^{-3}
ρ_L	Solution density	1248.93	kg m^{-3}

4. On-line dynamic optimization

Crystal growth dominant operation is often favored in batch crystallization processes. The crystal growth rate is a key process variable having a close relation with most of the product quality aspects. High crystal growth rates will typically result in more impurity uptake in the crystals, more liquid inclusions, as well as undesirable attrition and agglomeration. To suppress the latter phenomena that adversely affect the product quality, the supersaturation level in the crystallizer should be limited to the metastable region such that low crystal growth rates are attained at all times during the batch. This however leads to a loss in the batch productivity due to the low supersaturation levels in the crystallizer.

In order to be able to realize a trade-off between the fulfillment of product quality requirements and the maximization of batch throughput, the optimal control problem should be formulated such that an upper limit on the crystal growth rate is met throughout the batch run. The dynamic optimization problem is therefore defined as follows:

$$\min_{Q(t)} \frac{\int_0^{t_f} (100(G(t) - G_{\max})/G_{\max})^2 dt}{\int_0^{t_f} dt} \quad (9)$$

s.t. Eqs. (4) – (8)

$$Q_{\text{low}} \leq Q(t) \leq Q_{\text{high}}$$

where Q is the parameterized heat input profile, t_f is the batch time and G_{\max} is a conservatively chosen maximum crystal growth rate to avoid the formation of irregularly shaped crystals and limit the undesirable effects of high supersaturation levels ($G_{\max} = 2.5 \times 10^{-8} \text{ m s}^{-1}$). In fact Eq. (9) computes the optimal control action, i.e. heat input to the crystallizer, over a future time frame, the so-called control horizon. An inequality constraint is however imposed on the heat input; the lower limit Q_{low} is to ensure the survival of ground seeds during the initial phase of the batch, while the upper actuator constraint Q_{high} is due to physical limitations of the process. It is well evident that the optimal control problem stated in Eq. (9) expresses the desire to sustain the product quality by suppressing excessive growth rates. This implies that the maximization of the batch productivity is sought as the secondary interest.

The optimization problem is solved in GAMS simulation environment using CONOPT3 solver, which is well suited for the solution of constrained optimization problems by means of non-linear programming (NLP) algorithms. The optimal control problem is converted to an NLP problem via simultaneous optimization approach (Huesman et al., 2007) in which all the differential equations are transformed to algebraic equations by parameterization of the state and input trajectories. The implicit Euler scheme is utilized for discretization of the variables due to its unconditional numerical stability. The input and state profiles consist of 180 elements spanned over a prediction horizon of 3600 s, which is equivalent to the control horizon in this case.

The feedback control system depicted in Fig. 1 is devised to use the dynamic optimizer for real-time implementations. In this framework, the dynamic optimization problem is continuously solved on-line in a receding horizon mode (Maciejowski, 2002) such that the deviations of the process output, i.e. crystal

growth rate, from the reference trajectory, i.e. G_{\max} , are kept as small as possible in the presence of plant-model mismatch and process uncertainties. Thus, an observer is utilized to estimate the initial conditions x_{est} based on the process model and the available process measurements y_{meas} . The estimated states are used to initialize the optimization problem recursively at regular time intervals. The observer also enables one to estimate the supersaturation profile, i.e. solute concentration, for which actual measurements are not obtainable. In this study, an extended Luenberger-type observer designed on the basis of the moment model (Kalbasenka et al., 2006) is used to reinitialize the dynamic optimizer every 120 s, when new information on system states becomes available through CSD and crystal content measurements. Then every 20 s, the first element of the optimal operating policy, i.e. heat input profile, is taken as the set-point value and applied to the process using a conventional PI controller which takes the control action u to eliminate the difference between the process value of the heat input Q_{pv} and the set-point Q_{sp} . The PI controller is embedded in a Distributed Control System (DCS, CENTRUM CS3000, Yokogawa, Japan) that forms the basic control layer. An OPC (OLE (Object Linking and Embedding) for Process Control) communication interface (IPCOS, The Netherlands) facilitates the timed signal exchange among the various modules of the control architecture.

5. Results and discussion

5.1. Model validation

It follows from the model description given in Section 3 that the dynamics of the system under investigation are governed by a set of differential algebraic equations, i.e. Eqs. (4)–(8). It is expected that the moment model provides an adequate description of the process for the intended control application. This is due to the fact that large seed loads are used in the batch experiments which result in relatively low supersaturation levels (Doki et al., 2002). Under these conditions, the effect of secondary nucleation is minimized and, consequently, the crystal growth mainly dictates the evolution of the crystal size distribution throughout the batch. This implies that the CSD is often uni-modal and, therefore, can be well represented by the mean crystal size and the CSD width obtained from the moment model. The use of the moment model is also motivated by the high computational burden required to numerically solve the population balance equation; this may render the real-time implementation of the proposed model-based control strategy computationally infeasible.

In order to ensure that the moment model is an adequate representation of the process at hand, model validation is performed. The moments of the measured crystal size distribution and the model predictions are depicted in Fig. 2. The measured moments are calculated from the crystal volume density distributions and the crystal volume fraction data obtained at regular sampling time intervals during the experiment. As can be inferred from Fig. 2, the measured and simulated moments of the crystal size distribution are in good agreement except for the zeroth and the first moments. A satisfactory fit is also achieved for the mean crystal size defined as the quotient of m_4 to m_3 .

The poor fit quality obtained for the first two leading moments of the CSD is mainly attributed to the limitations

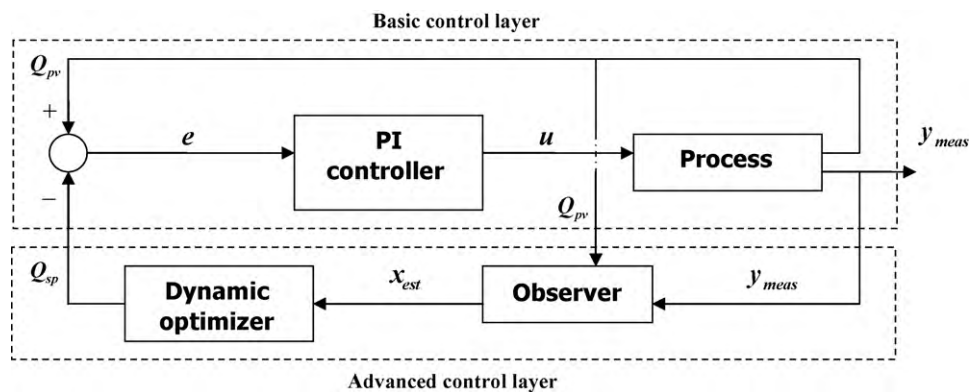


Fig. 1 – Block diagram of the on-line optimal control system.

of the CSD measurement technique. The laser diffraction CSD measurement device has a low sensitivity towards the smallest crystals that are small in volume but large in numbers. This implies that the measured zeroth moment of the CSD, which corresponds to the number of crystals present in the sample, is to a large extent unreliable.

5.2. Experimental implementation of the control strategy

The performance of the proposed model-based control strategy is experimentally examined by several real-time implementations on the 75-l draft tube crystallizer described

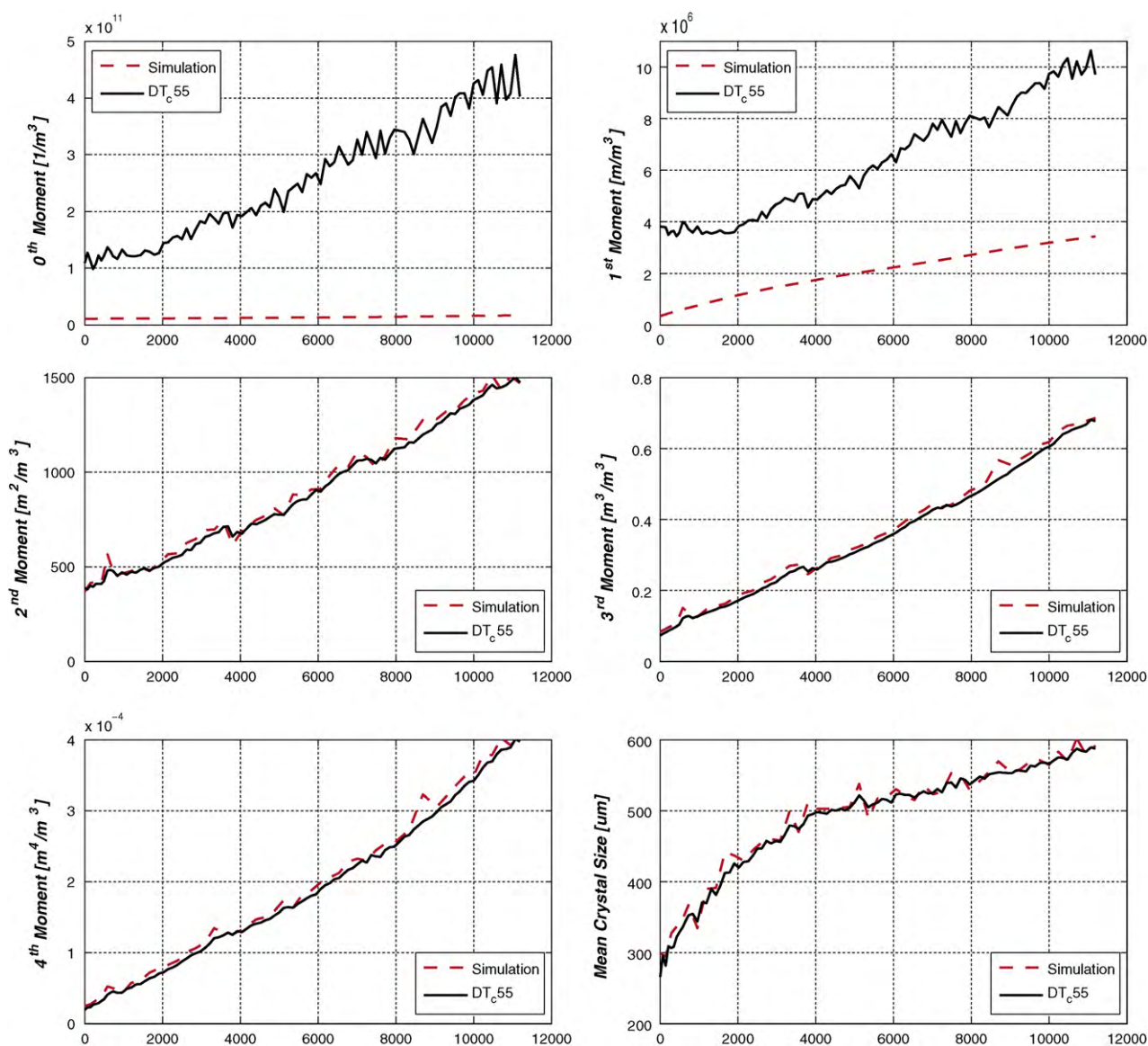


Fig. 2 – Validation of the moment model.

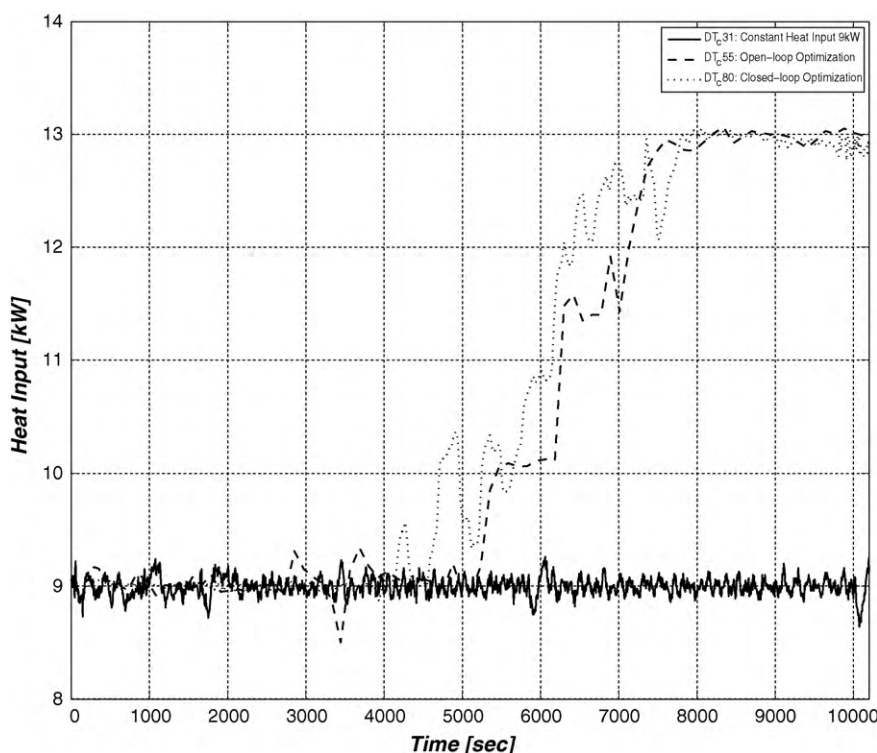


Fig. 3 – Heat input profiles.

in Section 2. As the product quality in seeded batch runs is predominantly determined by the crystal growth rate, variations of the crystal growth rate in relation to different heat input profiles are investigated in various experiments. The settings of the seeded fed-batch evaporative crystallization experiments are listed in Table 2.

The first three experiments, namely DT_{c31} , DT_{c55} and DT_{c80} , aim at revealing the superiority of the on-line computation of the optimal control profile over the open-loop implementation of the off-line optimized profile. Figs. 3 and 4 depict the heat input and growth rate profiles in the seeded batch runs, respectively. As can be seen, when the heat input to the crystallizer is kept constant at 9 kW throughout the experiment DT_{c31} , the crystal growth rate steadily decays being unable to fulfill its constraint, represented by the dash-dotted line in Fig. 4. This implies that a control action has to be taken in order to facilitate an effective crystal growth rate control during the batch runs. The optimal operating policy is, therefore, computed in an off-line setting and manually applied to the process as a time-varying set-point of the heat input PI controller during the experiment DT_{c55} . Fig. 4 shows that the growth rate is yet again unable to closely track its constraint due to the open-loop implementation of the optimal heat input trajectory.

The above discussed inability to fulfill the crystal growth rate constraint motivates the on-line computation of the optimal heat input trajectory in the experiment DT_{c80} . As shown in Fig. 4, when the crystal growth rate crosses the constraint at 4000 s, it is forced to follow the maximum growth rate by raising the heat input to the crystallizer. The constraint cannot however be tracked any longer as soon as the heat input reaches its upper bound of 13 kW at 8000 s and, consequently, the growth rate gradually drops while the heat input remains at its maximum admissible value. It is evident that the closed-loop implementation of the dynamic optimizer offers a better constraint tracking till actuation limitations render the optimal control of the batch process impossible. This superior performance owes to the feedback structure, as well as the receding horizon implementation of the control strategy that accounts for the plant-model mismatch and enables effective disturbance handling by state adaptation in the observer.

Nonetheless, Fig. 4 reveals that the growth rate constraint is not maintained in the initial phase of the batch since the heat input cannot be lowered below 9 kW. This is due to the hard constraint defined on the heat input, i.e. Eq. (9), to suppress possible dissolution of the inserted seeds (Kalbasenka et al., 2007). To further investigate the effect of the latter con-

Table 2 – Description of the seeded fed-batch evaporative crystallization experiments.

	DT_{c31}	DT_{c55}	DT_{c80}	DT_{c81}	DT_{c82}
Impeller frequency, rpm	450	450	450	450	450
Temperature, °C	50	50	50	50	50
Pressure, mbar	100	100	100	100	100
Heat input, kW m^{-3}	9.0	Manual	Optimizer ($Q_{low} = 9$ kW)	4.5	Optimizer ($Q_{low} = 2$ kW)
Seed fraction, μm	90–125	90–125	90–125	90–125	90–125
Seed mass, g	600	600	600	600	600
Seed preparation time, min	57	60	53	55	62
Relative supersaturation at seeding point	0.01627	0.00567	0.01103	0.00705	0.00683

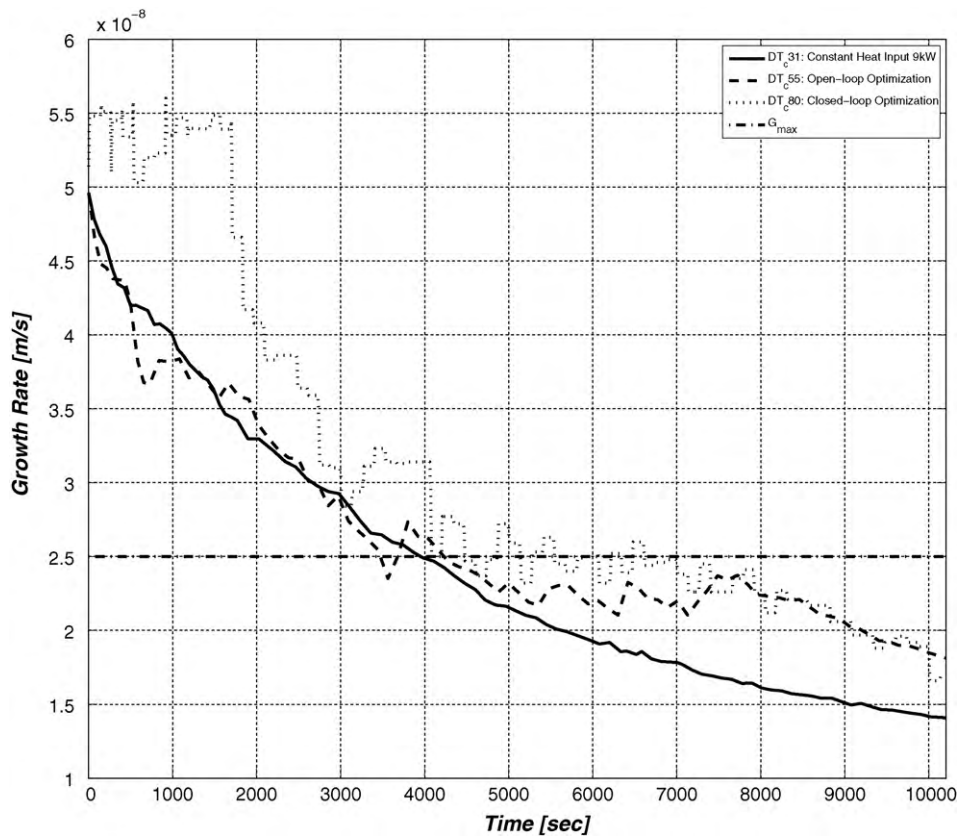


Fig. 4 – Crystal growth rate profiles.

straint on the product quality, namely the CSD properties, and to attain a more effective optimal control of the crystal growth rate, two more seeded batch experiments are carried out. Figs. 5 and 6 show that in experiment DT_{c81} , where the

seeds are introduced into the crystallizer at the heat input of 4.5 kW, the median and the width of the first measured CSD remain to a large extent similar to the previous batch runs. This suggests that the lower bound of the heat input can be

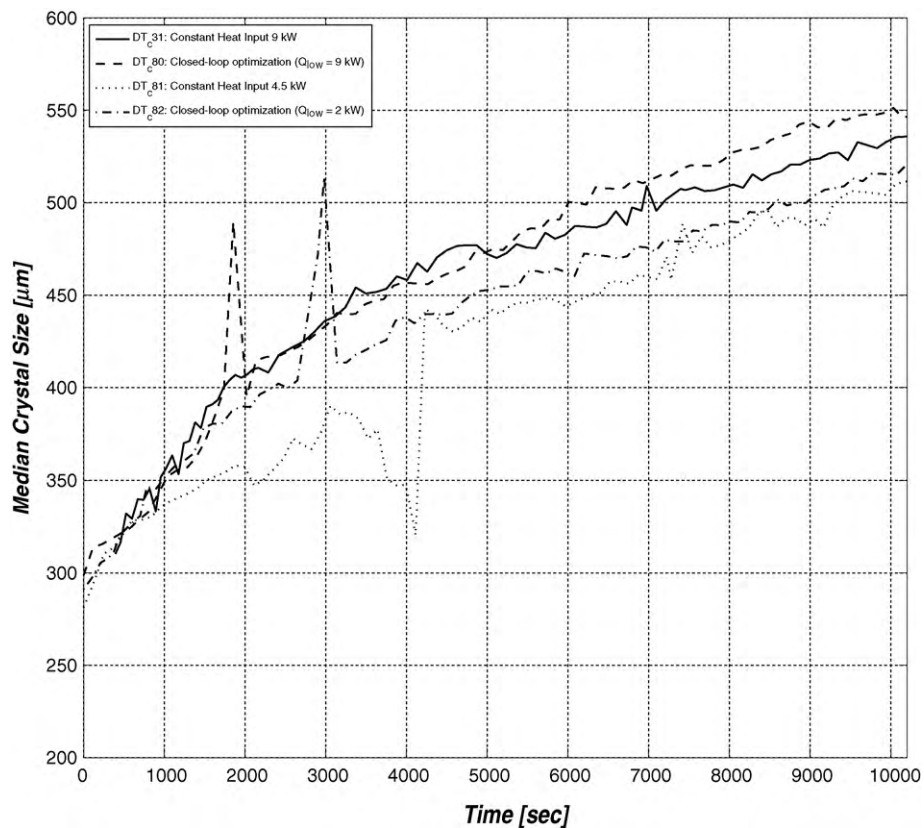


Fig. 5 – Median crystal size.

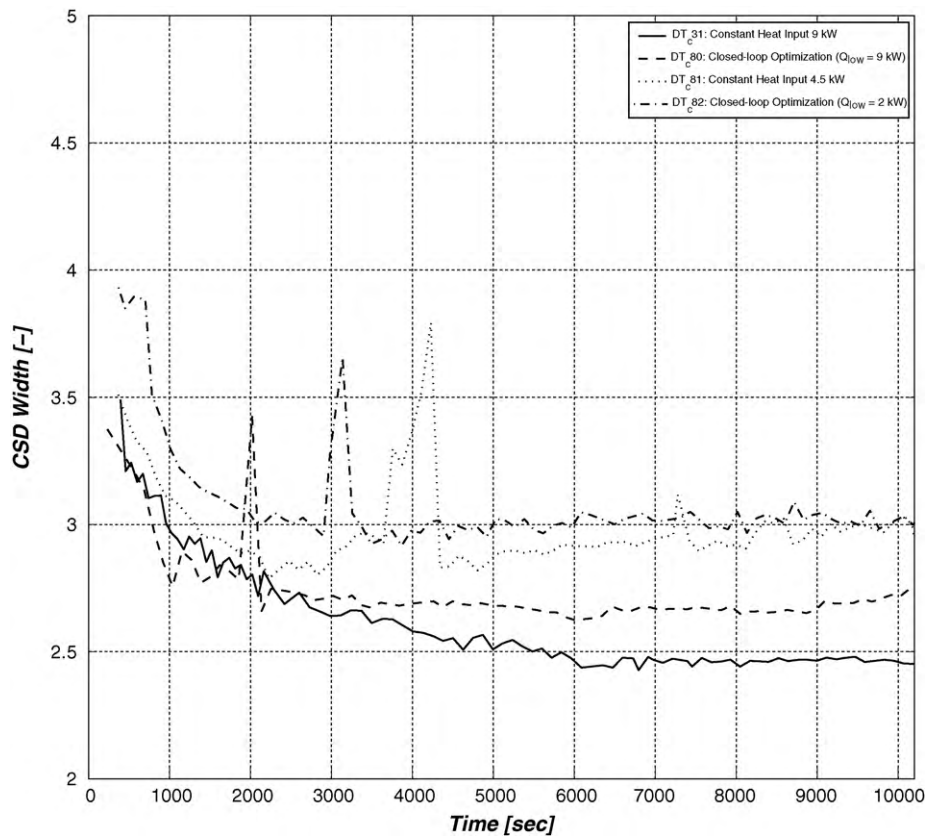


Fig. 6 – Width of the crystal size distribution.

further lessened as it is unlikely that the seeds dissolve when they are exposed to lower heat inputs.

In experiment DT_c82, the lower heat input bound is reduced to 2 kW. The heat input and the growth rate pro-

files corresponding to the closed-loop implementation of the dynamic optimizer subjected to the new constraint are shown in Figs. 7 and 8, respectively. In this batch run, the seeds are inserted into the crystallizer at the heat input of 4.5 kW; then

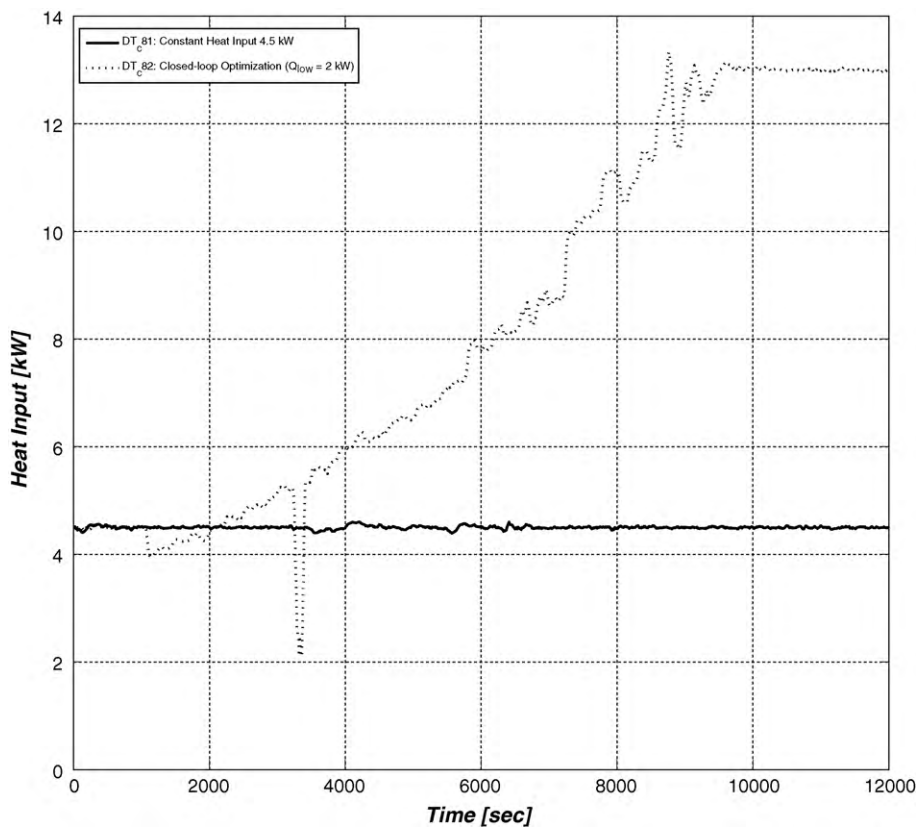


Fig. 7 – Optimal heat input profile throughout the batch.

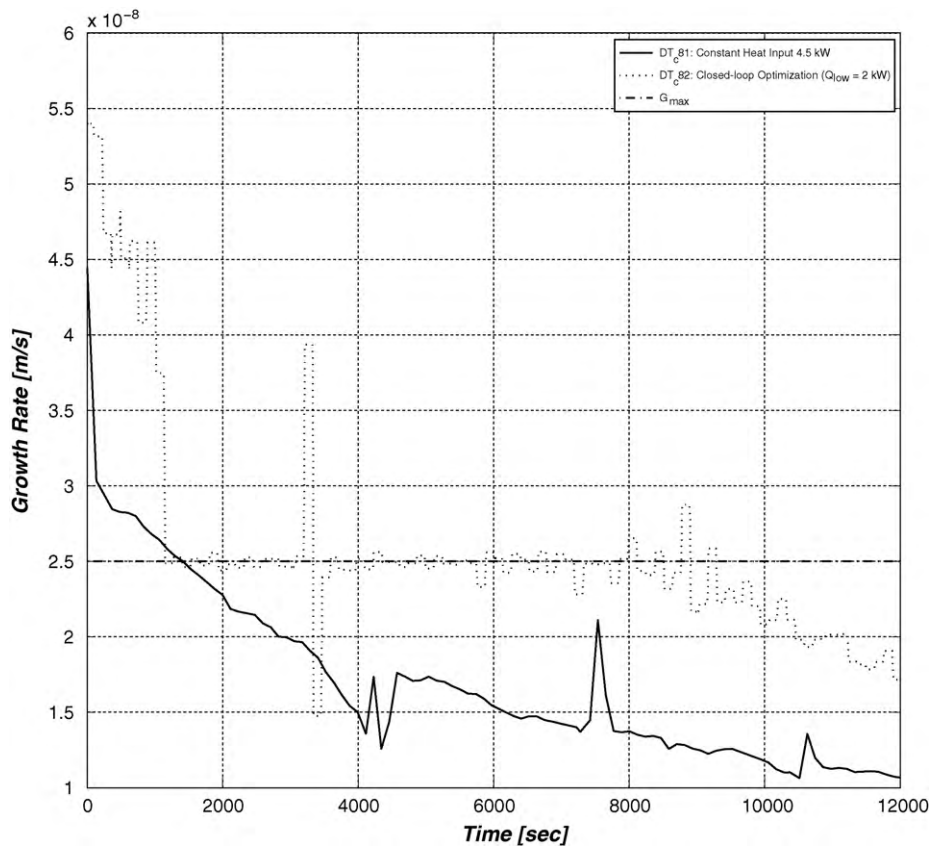


Fig. 8 – Optimal crystal growth rate profile throughout the batch.

having obtained 8 reliable CSD measurements to appropriately initialize the dynamic optimizer, the optimal control system is switched on. Fig. 7 shows that a control action is immediately taken to bring the crystal growth rate to its constraint

by decreasing the heat input to 3.9 kW. Subsequently, a fairly well growth rate constraint tracking is achieved till the heat input reaches its maximum admissible value, i.e. 13 kW. The effectiveness of applying the on-line optimal control strategy

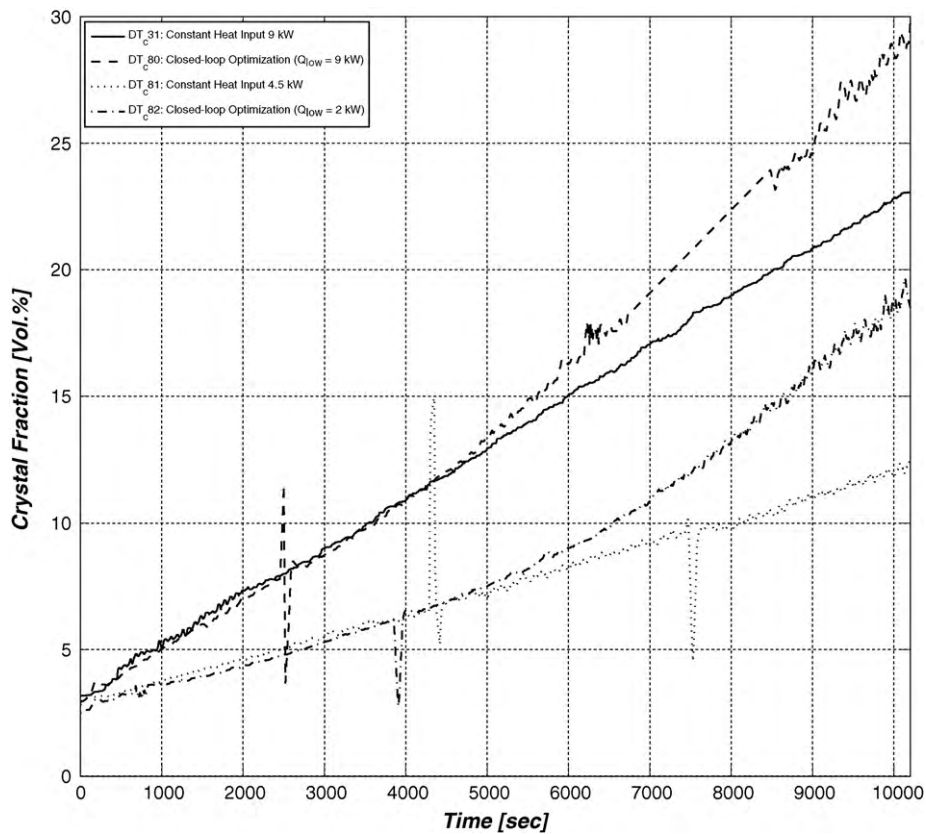


Fig. 9 – Batch crystal yield.

to achieve the maximum crystal growth rate in the course of a batch crystallization process can be clearly inferred from Fig. 8 that shows an uncontrolled process, namely the experiment DT_c81, leads to continuous violation of the maximum growth rate.

Fig. 9 reveals that real-time implementation of the dynamic optimizer substantially increases the batch productivity in comparison with the respective reference experiment with a constant heat input profile. This is due to the higher crystal growth rates obtained in the seeded batch run. The spikes in the crystal content measurements are due to the blockage of the product line of the crystallizer that is alleviated by rinsing the line with hot water. As shown in Fig. 9, reducing the lower heat input constraint adversely impacts the batch productivity. This effect can be justified by the superior product quality specifications, achieved by the tight crystal growth rate control throughout the batch run. However, these quality aspects may not be directly visible in the measured CSD characteristics, i.e. the median crystal size and the width of the distribution. It should be noted that the fulfillment of the product quality requirements in batch crystallization processes is often of greater importance than the maximization of the process yield.

The evolution of the median crystal size and the CSD width during the various experiments is depicted in Figs. 5 and 6, respectively. As can be seen, the seeded batch runs exhibit almost similar initial behavior in terms of the CSD characteristics. This is the result of the optimal seeding procedure that circumvents irreproducible start-ups due to uncertain initial conditions. Fig. 5 shows that the median crystal size achieved at the end of the batch runs to which the control strategy is applied remains almost identical to their respective reference experiments. Lowering the heat input constraint however results in a slight reduction in the product median crystal size due to a lower overall crystal growth rate in the course of the batch. In the experiments DT_c81 and DT_c82, the CSD width is also somewhat broader as shown in Fig. 6. This can be attributed to the lower supersaturation level at the seeding point which may possibly cause partial dissolution of the seeds.

6. Conclusions

In this paper a real-time dynamic optimization strategy for industrial batch crystallization processes is developed and experimentally validated on a 75-l evaporative draft tube crystallizer. The model-based controller aims to maximize the batch productivity without jeopardizing the product quality. The quality requirement is implemented as an upper constraint on the crystal growth rate that should be fulfilled at all times during the batch.

This study demonstrates that dynamic optimization is an effective control strategy for model-based optimal operation of batch crystallizers. It is shown that the open-loop implementation of the optimal profiles deteriorates their effectiveness mainly due to the plant-model mismatch and process uncertainties. Such shortcomings can to a large extent be accounted for by on-line computation of the optimal trajectories with feedback of the process states, estimated from on-line measurements. The results show that application of the proposed control policy allows the maximization of the production rate, while fulfilling the product quality requirements. Furthermore, it is revealed that the constraints to

which the optimal control problem is subjected may considerably suppress the optimal operation of the process. As shown, relaxing the input constraint leads to a far better control of the crystal growth rate, which in turn dictates the product quality.

In future, the current work will be extended to the optimal control of an 1100-l draft tube baffle crystallizer equipped with a fines removal loop that offers an extra degree of freedom to better control the CSD.

Acknowledgements

The work presented in this paper was carried out within the EUREKA/IS-project E! 3458/IS043074, called CryPTO (Crystalliser based Processing: fundamenTal research into mOdelling). The financial support of SenterNovem is gratefully acknowledged.

References

- Doki, N., Kubota, N., Yokota, M. and Chianese, A., 2002, Determination of critical seed loading ratio for the production of crystals of uni-modal size distribution in batch cooling crystallisation of potassium alum. *J. Chem. Eng. Jpn.*, 35: 670–676.
- Hu, Q., Rohani, S., Wang, D.X. and Jutan, A., 2005, Optimal control of a batch cooling seeded crystallizer. *Powder Technol.*, 156: 170–176.
- Huesman, A.E.M., Bosgra, O.H. and Van den Hof, P.M.J., 2007, Degrees of freedom analysis of economic dynamic optimal plantwide operation, In *Proceedings of the 8th International IFAC Symposium on Dynamics and Control of Process Systems Cancun, Mexico*, , pp. 165–170.
- Kalbasenka, A.N., Landlust, J., Huesman, A.E.M. and Kramer, H.J.M., 2006, Application of observation techniques in a model predictive control framework of fed-batch crystallization of ammonium sulphate, In *Proceedings of WCPT-5 Orlando, USA*,
- Kalbasenka, A.N., Spierings, L., Huesman, A.E.M. and Kramer, H.J.M., 2007, Application of seeding as a process actuator in a model predictive control framework for fed-batch crystallization of ammonium sulphate. *Part. Part. Syst. Charact.*, 24(1): 40–48.
- Landlust, J., Mesbah, A., Wildenberg, J., Kalbasenka, A.N., Kramer, H.J.M. and Ludlage, J.H.A., 2008, An industrial model predictive control architecture for batch crystallization, In *Proceedings of the 17th International Symposium on Industrial Crystallization Maastricht, The Netherlands*, , pp. 35–42.
- Lang, Y.D., Cervantes, A.M. and Biegler, L.T., 1999, Dynamic optimization of a batch cooling crystallization process. *Ind. Eng. Chem. Res.*, 38: 1469–1477.
- Maciejowski, J.M., (2002). *Predictive control with constraints*. (Pearson Education Ltd, London, UK).
- Mayrhofer, B. and Nyvlt, J., 1988, Programmed cooling of batch crystallizers. *Chem. Eng. Process.*, 24: 217–220.
- Mesbah, A., Kalbasenka, A.N., Huesman, A.E.M., Kramer, H.J.M. and Van den Hof, P.M.J., 2008, Real-time dynamic optimization of batch crystallization processes, In *Proceedings of the 17th IFAC World Congress Seoul, Korea*, , pp. 3246–3251.
- Miller, S.M. and Rawlings, J.B., 1994, Model identification and control strategies for batch cooling crystallizers. *AIChE*, 40: 1312–1327.
- Mullin, W. and Nyvlt, J.N., 1971, Programmed cooling of batch crystallizers. *Chem. Eng. Sci.*, 26: 369–377.
- Nowee, S.M., Abbas, A. and Romagnoli, J.A., 2007, Optimization in seeded cooling crystallization: a parameter estimation and dynamic optimization study. *Chem. Eng. Process.*, 46: 1096–1106.

-
- Randolph, A. and Larson, M., (1971). *Theory of Particulate Processes*. (Academic Press, New York, USA).
- Shi, D., El-Farra, N.H., Li, M., Mhaskar, P. and Christofides, P.D., 2006, Predictive control of particle size distribution in particulate processes. *Chem. Eng. Sci.*, 61: 268–281.
- Xie, W., Rohani, S. and Phoenix, A., 2001, Extended Kalman filter based nonlinear geometric control of a seeded batch cooling crystallizer. *Chem. Eng. Commun.*, 187: 229–249.
- Zhang, G.P. and Rohani, S., 2003, On-line optimal control of a seeded batch cooling crystallizer. *Chem. Eng. Sci.*, 58: 1887–1896.